Semiannual Progress Report

Submitted to: National Aeronautics and Space Administration
Langley Research Center
Hampton, Va 23665-5225
Attn: Dr. Robert C.Coston
Technical Officer, M/S493

Institution: Hampton University
Dept of Physics

Title of Research: Direct Solar-pumped Iodine Laser Amplifier

NASA Grant No.: NAG-1-441

Period Covered: March 1,88 - Aug 31,88

Principal Investigator: Kwang S. Han
Co-Principal Investigator: In H. Hwang
Research Associate: Larry V. Stock

Direct Solar-Pumped Iodine Laser Amplifier

Contents

Abstract

This semiannual progress report covers the period from March 1, 1988 to Aug 31, 1988 under NASA grant NAG-1-441 entitled "Direct solar-pumped Iodine laser Amplifier". During this period, XeCl laser which was developed earlier for an iodine laser oscillator has been modified in order to increase the output pulse energy of XeCl laser so that the iodine laser output energy could be increased. The electrical circuit of the XeCl laser was changed from a simple capacitor discharge circuit to a Marx system. Because of this improvement the output energy from the XeCl laser was increased from 60mJ to 80mJ. Subsequently, the iodine laser output energy was increased from 100 mJ to 3 mJ.

On the other hand, the energy storage capability and amplification characteristics of the Vortek solar simulator-pumped amplifier was calculated expecting that the calculated amplification factor is about 2 and the energy extraction efficiency is 26% due to the very low input energy density to the amplifier.

As a result of an improved kinetic modeling for the iodine solar-simulator pumped power amplifier, it is found that the $[I_2]$ along the axis of the tube affects seriously the gain profile. For the gas i-C_3F_7I at the higher pressures, the gain will decrease due to the $[I_2]$ as the pumping intensity increases, and at these higher pressures an increase in flow velocity will increase the gain. In addition, there is an optimum medium for a specific velocity. These gain calculations is the first step in developing a kinetic model of the MOPA system. Details of these gain calculations are reported.

A. Introduction

The development of a high power solar-pumped laser is an ultimate goal of various solar energy research laboratories around the world. The ground-based solar laser research is currently active for the development of high power laser system. The ground-based solar laser could provide very cheap laser photons which could be applied in various industries.

On the other hand the space-based solar laser has promising applications such as the laser propulsion of space vehicle and the energy transfer between spacecrafts. A continuous wave (CW) laser has the best applicability for the above mentioned applications. However, among the various laser materials, only two kind of laser materials were successfully employed in the CW solar laser-pumped laser. The one is Nd doped solid laser materials [1,2] and the other is iodine containing organic compounds [3]. The solid material has some limitations for the applications in the solar-pumped laser such as the heat removal from the laser rod and the self-focussing effect when operated at high power level. More serious limitation for the application in the space-based solar laser is the limited size (several inches) of the crystals available. In general the longer the material length is, the lower the threshold pump power for a given cavity is.

In contrast to the solid laser material, gaseous laser materials have no thermally induced self-focussing problem and the heat removal is easily accomplished by circulating the laser medium. The main disadvantage of the gas medium is the low spectral utilization of the

solar irradiance. Generally, the absorption band of the gaseous material is very narrow as compared with the solid laser materail. Although the CW solar-pumped laser research has been successful in various laboratories because of the limitation by the kinetics of the laser materials used and weak solar irradiance, a single laser oscillator can hardly produce very high output power. The applications to obtain 1 MW output with an iodine laser show that the tube of the laser oscillator should be about 10m and the diameter about 2 m [4]. The laser optics for such a large laser system will be very heavy, and the developmental cost of such a laser system for space applications will require a major commitment by nation.

Introducing a Master Oscillator Power Amplifier (MOPA) system, the heavy laser optics can be eliminated and high peak power can be obtained with a moderate size of the amplifier. To make a MOPA system successful, the amplifying medium should behave a long excited lifetime so that the medium could store a large amount of energy during the period of pumping. Among the various laser materials, atomic iodine has a suitable excited state lifetime of the amplifying medium of the MOPA system. The excited state lifetime of the atomic iodine is about 130 ms for an isolated atom. However, the excited state lifetime is greatly reduced when the iodine atom is in a gas medium because of the perturbation from the parent gas. But the previous experimental result confirms the considerably long energy storage time ($\approx$ 1 ms) in a practical iodine laser amplifier [5]. Moreover, the iodine laser kinetic study shows that the population inversion inside laser tube builds up until 0.2 sec from

the beginning of the irradiation of the solar radiation when the pressure of the iodine containing chemical is very low (≈2 Torr) [6].

Once the energy storage reaches its maximum by pumping from the solar radiation, the stored energy is extracted by a laser beam from an iodine laser oscillator in the MOPA system. If the pulse duration from the oscillator is short, then the peak power extracted from the amplifier is high. The standard method for obtaining the short pulse from an oscillator is Q-switch or mode-locking but the oscillator system with Q-switch or mode-locking is very complicated. The way of obtaining short pulse from an iodine laser is to pump the iodine laser oscillator with an excimer laser is usually a few 10 nsec. Because of this short pump pulse the iodine laser pulse duration is below a few 10 nsec. The study of the excimer laser-pumped iodine laser was conducted earlier by the Quantenoptik group in Max Plank Institute [7]. They used i-C_3F_7I as the laser material, and both XeCl and KrF laser were used as the pump source. The pulse duration from 2.6 nsec to 12 nsec was obtained by varying the resonator length.

In the present research, a different laser material t-C_4F_7I is used. This material has about 2.5 times larger absorption cross section at XeCl laser line (308 nm) compared with that of i-C_3F_7I. To increase the output of the previously fabricated XeCl laser system for an increased iodine laser output, the electrical circuit of the XeCl laser system was modified from a simple mesh-capacitor discharge circuit to a Marx system having voltage multiplication. After this modification, the iodine laser output

energy reached 3 mJ sufficient for incorporating with the Vortek solar-simulator pumped amplification tube, and forming a simulated solar-pumped MOPA system. In the following sections, the improvement of XeCl laser will be described. And also the energy storage capability of the Vortek solar simulator-pumped amplifier will be calculated and thus the experimental result could be compared.

B. Improvement of XeCl Laser and Iodine laser oscillator

In the previous research, XeCl laser system was fabricated with a simple-mesh capacitor discharge circuit as the driver. The maximum output energy per pulse was only 60 mJ. To improve the XeCl laser output, a two-stage Marx system was formed to replace the simple discharge circuit. The schematic diagram is shown in Fig.1 of Appendix. As shown in the figure, the two 40 nF energy storage capacitors are charged through the resistors by the high voltage power supply. Once the trigger pulse is applied to the spark gap switches, the two energy storage capacitors are connected in series and thus the voltage across the two laser electrodes doubles the voltage of the single energy storage capacitor.

The preionizer in the XeCl laser chamber assists the discharge uniformity. The uniform discharge is very important to obtain a spatially uniform laser output. Though the preionizer was installed in the laser chamber to increse uniformity of the laser discharge, the electrical discharge transits to arc when the XeCl was operated at higher voltage. In the course of experiment, it was found that the addition of Ar gas in the

laser gas mixture improved the discharge uniformity, and thus the laser produced a spatially uniform output over 25 kV of charging voltage. The total pressure of the laser gas mixture ratio was HCl:Xe:Ar:He = 0.2%:5.9%:19.5%:74.4%.

With these improvements, the XeCl laser produced 80 mJ pulse energy at the charging voltage of 25 kV. The efficiency of the fabricated XeCl laser is calculated to be about 0.32% which is quite low compared with commercial products (≈1%). However, the output beam (1 x 2 cm^2) has a quite good uniformity.

The iodine laser oscillator pumped by the XeCl laser generated 3 mJ output energy when a 5 cm long laser tube was filled with t-C_4F_9I at the pressure 80 Torr and the output mirror reflectance was 85%. The detailed experimental setup and results are described in the Appendix which is submitted to the Optics Communication for publication.

C. Amplification by Vortek simulator-pumped Amplifier

The amplification characteristics of the solar simulator pumped amplifier is determined by the population inversion in the simulator tube. The order of magnitude estimation of the population inversion is now possible by using the previous experimental results [3]. The equivalent solar irradiance at the surface of the amplifier is about 1300 S. C. (solar constant) when the Center's Vortek solar simulator is operated at the current of 300 A [3]. Also the CW laser experiment shows that the

optimum pressure in the laser tube is about 20 Torr when the flowing speed of the iodide in the laser tube is about 20 m/sec.

The quantum yield of the iodides which are used in the iodine laser experiment is approximately unity in the spectral range of absorption. Thus, the absorbed photons in the iodine produce the excited atomic iodine only. From this fact, the photodissociation rate is equivalent to the pump rate to the excited level of the atomic iodine. The pump rate is now calculated as

$$W_p = A \cdot (S.C.) \cdot \int_0^{\infty} F(\lambda)[1-\exp\{-\sigma_a(\lambda)ND\}]d\lambda \qquad (1)$$

where A is the surface area of the laser tube, (S.C) is the solar constant on the surface od the laser tube, F(l) is the photon flux in the spectral range l and l + dl, $\sigma_a(l)$ is the absorption cross section of the iodide molecule in the spectral range l and l + dl, N is the number density of the iodide molecule inside the laser tube and D is the diameter of the laser tube. If the diameter of the laser tube is assumed to be 2 cm, the length to be 20 cm, and the iodide fill pressure to be 20 Torr, then the pump rates calculated by the equation (1) for the various iodides are shown in Table 1.

As shown in table 1, t-C_4F_9I can be pumped almost twice the rate of C_3F_7I at the same solar concentration that is a definite advantage in the solar pumped iodine laser system.

Table 1 The pump rates of various iodides

The tube diameter is 2 cm and the tube length 20 cm. The pressure inside the tube is 20 Torr and the pumping intensity on the surface of the laser tube is 300 solar constant.

Iodide	C_2F_5I	n-C_3F_7I	I-C_3F_7I	t-C_4F_9I
Total pump rate(No./sec)	1.36×10^{20}	1.96×10^{20}	1.98×10^{20}	3.76×10^{20}
Pump rate per unit volume (No./cm^3)	2.16×10^{18}	3.12×10^{18}	3.15×10^{18}	5.98×10^{18}

The number of the excited atomic iodine is now calculated by multiplying the pump rate with the pumping time. When the iodide gas flows with velocity of 20 m/sec through the 20 cm long amplifier tube, the average pumping time is 10 msec. Thus, the excited atomic iodine density could be $3.12\times10^{16}/cm^3$ for the case of n-C_3F_7I which will be used in next experiment. This calculation shows the upper limit of the excited atomic iodine density because the quenching process by the parent molecules is not taken into account. The quenching rate of the excited atomic iodine by the parent molecule is rather high [$\approx2\times10^{-16}$ cm^3/sec for n-C_3F_7I] and thus the excited atomic iodine density in the amplifier tube will be far less than the value $3.12\times10^{16}/cm^3$. Moreover, the quenching by the molecular iodine will also reduce the excited atomic iodine density in the laser tube. Due top these quenching processes, the achievable population inversion density is expected to be about 1.0×10^{16} $/cm^3$ which is about 1/3 of the upper limit of the population inversion.

The amplification by the amplifier which contains the population inversion density ΔN is given by

$$E_{out} = E_s \ln[1 + \{\exp(E_{in}/E_s) - 1\}\exp(\sigma \Delta N\, l)] \qquad (2)$$

where E_{out} is the output energy density (J/cm^2), and E_s the saturation energy density which is given by $E_s = (a/b)(h\nu/\sigma)$, E_{in} is the input energy density (J/cm^2), σ is the stimulated emission cross section and l is the length of the amplifier. The coefficient a/b in the saturation energy density is dependent on the incident pulse because of the relaxation times of the upper and lower laser level of the atomic iodine. The saturation energy density for the present experiment is calculated to be 15.8 mJ/cm^2 because the stimulated emission cross section of the atomic iodine at the n-C_3F_7I pressure of 20 Torr is 4.3×10^{-18}cm^2 and a/b is about 0.45.

The output energy from the XeCl laser pumped iodine laser oscillator is about 3 mJ as shown in the appendix. If the oscillator output fills a circular cross section of diameter 1 cm when the beam enters to the amplifier, then the input energy density E_{in} is 3.8 mJ/cm^2. Substituting the values of parameters into the equation (2), the output energy density is calculated. The calculated output energy density is 7.8 mJ/cm^2 and the total energy which can be obtained from the amplifier output is 6.2 mJ. Thus the amplification factor which is defined by (energy output)/(input energy) is expected to be about 2.

The stored energy in the volume which is swept by the incident beam is calculated by

$$E_{st} = h\nu\ \Delta N\ V \qquad (3)$$

where V is the volume swept by the incident beam. The stored energy in the amplifier volume calculated by the equation (3) is 23.7 mJ. Therefore, the energy extraction efficiency is only 26%. This low energy extraction efficiency is due to the use of the very low energy from the iodine laser oscillator, indicating a need of a higher output oscillator for improvement.

The experimental setup for the measurement of the amplification characteristics of the Vortek solar simulator pumped amplifier is described in Fig. 1. The laser output from the XeCl laser pumped iodine laser oscillator is to be passed through the amplifier tube. The distance from the laser oscillator to the entrance of the amplifier is about 8 m. The divergence of the output beam from the oscillator is about 5×10^{-3} radian so that a beam collimator is expected to be used in the beam path to reduce the beam size in front of the amplifier tube. The amplification will be measured by comparing the input energy to the amplifier and the output energy from the amplifier.

References

[1] C. G. Young, Applied Optics 5, 993 (1966)

[2] K. S. Han, I. H. Hwang, K. H. Kim and L. v. Stock Progress Report, NASA Grant NAG-1-441 (1988)

[3] J. H. Lee, M. H. Lee and W. R. Weaver, Proceedings of the International Conference on Lasers, '86, page 150 R. W. McMillan Ed., STS Press, Mclean VA (1987).

[4] R. J. Young, G. H. Walker, M. D. Williams, G. L. Schuster and E. J. Conway, NASA Technical Memorandeum 4002 (1987).

[5] I. H. Hwang, J. H. Lee and M. H. Lee, Optics Comm. 58, 47 (1986).

[6] V. Yu. Zalesskii, Sov. J. Quant. Electron. 13, 701 (1983).

[7] E. Fill, W. Skrlac and K. J. Witle, Optics Comm. 37 , 123 (1981).

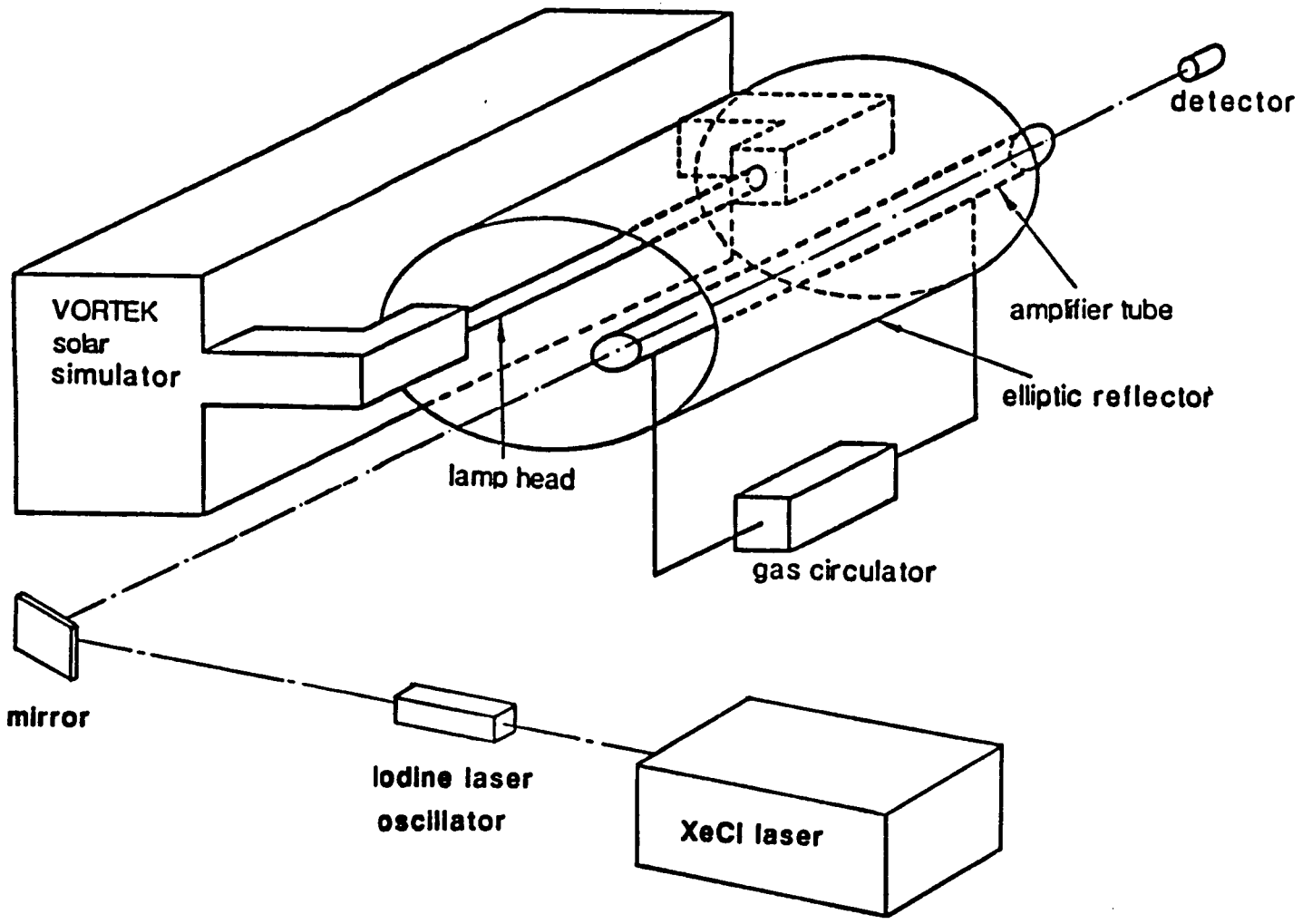

Fig. 1. Experimental set up for the measurement of the amplification of the Vortek solar simulator pumped amplifier.

Appendix; A paper submitted to Optics Communication for publication. 1

XeCl Laser Pumped Iodine Laser Using t-C_4F_9I

In Heon Hwang, Kwang S. Han
Department of Physics, Hampton University
Hampton, VA 23668

Ja H. Lee
NASA Langley Research Center, MS/493
Hampton, VA 23665-5225

Abstract

An iodine photodissociation laser using t-C_4F_9I as the active material was pumped by a XeCl laser. An iodine laser output energy of 3 mJ with pulse duration of 25 ns was obtained when the pumping pulse energy was 80 mJ, the iodide pressure was 70 torr, and the reflectance of the output mirror was 85%. The high pumping efficiency and low threshold pump power achieved in this experiment are attributable to the high absorption cross section at the pump laser wavelength (308 nm) of the iodide used.

I. Introduction

Since the atomic iodine photodissociation laser was discovered by Kasper and Pimentel in 1964 [1], numerous research efforts have concentrated on this laser to increase the power level needed for laser fusion [2,3]. The fusion-experiment-oriented iodine laser is constructed in a master-oscillator power-

amplifier (MOPA) architecture [4]. The amplifiers and the oscillator of the iodine laser are usually pumped by short pulse flashlamps.

The iodine laser is also being considered as a direct solar pumped laser for space applications such as the laser propulsion for an orbital transfer vehicle. The first solar simulator pumped iodine laser was reported in 1981 by Lee, et. al. [5]. This laser was operated in quasi-continous-wave mode. After this report, various iodine compounds were tested and evaluated as candidates for direct solar pumped laser materials [6,7,8].

Although many space applications are best served by a continuous wave (CW) laser a continuously pulsed laser also has good applicability in space especially for laser propulsion. If weak pumping exists, such as solar radiation pumping of laser materials, use of a MOPA system is essential for obtaining high peak power when the laser material has a long upper-state lifetime like an iodine atom. In previous research, the feasibility of the oscillator-amplifier scheme was proposed and tested for the solar pumped iodine laser [7,9].

The iodine laser oscillator must generate temporally smooth and short pulses in order to be incorporated in the MOPA system. In the fusion-oriented iodine laser experiment, the short pulse is provided by mode-locking of the flashlamp-pumped oscillator. However, the repetition rate of the flashlamp-pumped oscillator is usually very low (<5Hz), and the mode-locking devices are generally complicated.

An excimer laser pumped iodine laser oscillator was demonstrated by Fill et. al. [10]. In their experiment, a 500-mJ excimer laser was used for the pumping of the iodine laser, and a temporally smooth laser pulse with duration from 2.6 ns to 12 ns was obtained by using i-C_3F_7I as the laser material.

In this report, a XeCl laser pumped iodine laser using t-C_4F_9I is described. This laser oscillator has a much higher efficiency and a lower threshold pump power then the system using i-C_3F_7I. The laser output energy dependence on the gas-fill pressures and on the reflectances of the output mirrors are measured for both longitudinal and transverse pumping.

II. XeCl Eximer Laser

A laboratory built XeCl laser was used for the pumping of the iodine laser in this experiment. The electrical circuit of the XeCl laser is shown in Fig. 1. The main discharge was energized by a two-stage Marx generator. The capacitance of each stage is 40 nF. A pyrex tube with an I. D. of 0.1 m and a length of 0.66 m was used as the laser chamber. The two brass electrodes were rounded so as not to develop an arc discharge in the discharge volume. The width of the electrodes was 20 mm, and the length was about 0.45 m. The separation between the two electrodes was 20 mm. Seventeen pairs of arc arrays were located beside the electrodes so that the discharge volume could be preionized uniformly.

The optimized gas composition was HCl: Xe: Ar: He = 0.2% : 5.9%: 19.5%: 74.4% at a total pressure of 2 atm. The addition of Ar improved the discharge uniformity at the higher operating voltage. The XeCl laser was operated in a sealed-off mode. No significant reduction of the laser output energy was shown for a few hundred discharges.

The optical resonator of the XeCl laser was composed of a full reflector with a radius of curvature of 5 m and a flat partial mirror with a reflectance of 30%. All the mirrors were coated outside so that the mirror surfaces could not be damaged by the volatile discharge products. The two laser mirrors were

separated about 0.75 m. A spatially uniform laser output in a cross section of 0.7 x 2 cm^2 was obtained with this optical resonator.

When the XeCl laser was operated at the charging voltage of 25 kV, the output energy was 80 mJ per pulse. If the charging voltage was increased, the laser output was also increased, but an arc discharge was developed between the electrodes. Thus, operation above 25 kV was not pursued.

The output energy was measured with a calorimeter. The output pulse shape of the laser output was measured with a Si PIN photodiode with the glass window of the photodiode removed. The removal of the glass window improved the near UV response of the diode. A typical laser pulse is shown in Fig. 2. The half width (FWHM) of the XeCl laser pulse was about 25 nsec, and no significant variation of the laser pulse shape was found for prolonged operation.

III. Iodine Laser Experiment.

The iodide used in this experiment was t-C_4F_9I (perfluoro-tertiary-butyl iodide). This chemical was chosen mainly due to the high absorption cross section at the wavelength of XeCl laser light (308 nm). The published data [17] show that the absorption cross section of t-C_4F_9I at 308 nm is about 3.6 x 10^{-19} cm^2 [7]. Also, t-C_4F_9I has shown good chemical reversibility in a flashlamp-pumped system [6,7], and thus the iodine molecule buildup in the laser cell is minimized. The main disadvantage of this iodide is the low vapor pressure (~ 85 torr) at room temperature. The other chemical kinetic properties are nearly the same or better than the other commonly used perfluoroalkyl iodide in flashlamp-pumped experiment [7]. The quantum yield of excited atomic iodine in the UV photodissociation is nearly unity [11].

A quartz cuvette with a square cross section of 1 cm^2 and length of 50 mm was used as the iodine laser cell. The windows of the laser cell were nearly perpendicular to the optic axis of the laser cell. Both longitudinal and transverse pumping of the iodine laser were employed.

When the iodine laser was pumped longitudinally, a dichroic mirror was used to introduce the XeCl laser light into the iodine laser cell. The dichroic mirror transmitted about 80% of the XeCl laser light and fully reflected the iodine laser light. The XeCl laser light was directed through the dichroic mirror and was focused into the center of the laser cell by a quartz circular lens of focal length 0.2 m. The output pattern of the iodine laser was monitored on a carbon-paraffin paper. A typical laser output pattern was an ellipse with minor diameter 1 mm and major diameter 4 mm when the gas pressure in the cell was 80 torr and the reflectance of the output mirror was 85%.

When the iodine laser was pumped transversely, a quartz cylindrical lens of focal length 0.3 m was used to focus the XeCl laser light into the iodine laser cell. Because of the long focal length of the focusing lens, the laser output pattern was a long rectangle with an area of 1 x 10 mm^2.

The TEM mode pattern was not analyzed in either experiment, and no attempt was made to operate the iodine laser in the TEM_{00} mode. The output energy dependences on the gas fill pressure at different output mirror reflectances are shown in Figs. 3 and 4. As shown in Fig. 3, there is an optimum iodide pressure for each output mirror reflectance for the longitudinal pumping. However, for the transverse pumping, the laser output energy increases monotonically with the t-C_4F_9I pressure as shown in Fig. 4. The results in Figs. 3 and 4 were taken when the laser was operated at 2-Hz

repetition rate. When the pulse repetition rate was increased to 5 Hz, the laser output energy per pulse was reduced slightly (~ 10%) due to the reduction of the XeCl laser pump energy.

A typical laser pulse shape detected by a pyroelectric detector of the iodine laser output is shown in Fig. 5. The half width (FWHM) of the pulse is about 25 nsec. The iodine laser onset is delayed from the XeCl pump laser and occurs at the end of the pump pulse. This pulse shape is nearly the same for both pumping geometries.

IV. Discussion

In this experiment, a XeCl laser pumped iodine laser was developed and tested by using t-C_4F_9I as the laser material. This lasant t-C_4F_9I has larger absorption cross section at the XeCl laser line compared with other iodides used in the laser experiment such as i-C_3F_7I. The large absorption cross section allows the high utilization of pumping energy in short gain length and low pressure operation of the iodine laser. The low-pressure operation of the iodine laser is suitable for single longitudinal mode output because of the reduced pressure broadening of the gain profile. The single-longitudinal mode operation of the laser oscillator is necessary to obtain a temporally smooth pulse.

The iodine laser described in this report was operated up to 5 Hz, which was limited by the power supply of the XeCl laser. Further increases of the repetition rate can be made by scaling up the pump laser system. The iodine laser was operated in a sealed-off mode. There was no significant reduction of the laser output energy after a few hundred pumpings with a single fill of t-C_4F_9I in the laser cell. There was also no noticeable change in the t-C_4F_9I gas after a few hundred pumpings and no deposits on the wall of the laser cell

(contrary to the report of Ref. 10 where i-C_3F_7I was used). This may be attributable to the superior chemical reversibility of the iodide used.

V. Conclusion

A XeCl laser that pumped an iodine laser oscillator was developed using t-C_4F_9I as the laser material, and a 3 mJ laser output energy was obtained with only 80 mJ pumping energy. Compared with previous results, the pumping energy was dramatically reduced in this experiment. The pumping efficiency (i.e., the ratio of the iodine laser energy and the XeCl laser energy) was 3.75%. This experiment also demonstrated a repetitive operation of the iodine laser oscillator with a stable output. Since the threshold pumping energy (20 mJ) is low for t-C_4F_9I, a moderate size XeCl laser may suffice for pumping the high-repetition-rate iodine-laser oscillator required for solar pumped master-oscillator power-amplifier systems.

Acknowledgement

This work is supported in part by NASA grant NAG-1-441. We thank Fred M. Whitehead for his assistance in setting up the XeCl laser.

References

1. J. V. V. Kasper and G. C. Pimentel, Appl. Phys. Lett. 5, 231 (1964).

2. G. Brederlow, E. Fill and K. J. Witte, "The High-Power Iodine Laser," Springer-Verlag, New York, N. Y. (1983).

3. S. B. Kormer, Izvestiya Akademii Nauk SSSR. Seriya Fizicheskaya 44, 2002 (1980).

4. K. J. Witte, Czech. J. Phys. B34, 790 (1984).

5. J. H. Lee and W. R. Weaver, Appl. Phys. Lett. 39, 137 (1981).

6. J. H. Lee, J. W. Wilson, T. Enderson, D. H. Humes, W. R. Weaver and B. M. Tabibi, Optics Comm. 53, 367 (1985).

7. B. M. Tabibi, M. H. Lee, J. H. Lee and W. R. Weaver, Proceedings of the International Conference on Lasers '86, pp. 144-149 (1986).

8. R. J. DeYoung, IEEE . J. Quant. Electron. QE-22, 1019 (1986).

9. I. H. Hwang, J. H. Lee and M. H. Lee, Optics Comm. 58, 47 (1986).

10. E. Fill, W. Skrlac and K. J. Witte, Optics Comm. 37, 123 (1981).

11. A. B. Alekseev, A. M. Pravilov, I. I. Sidorov and V. A. Skorokhodov, Sov. J. Quantum Electron. 17, 1539 (1987).

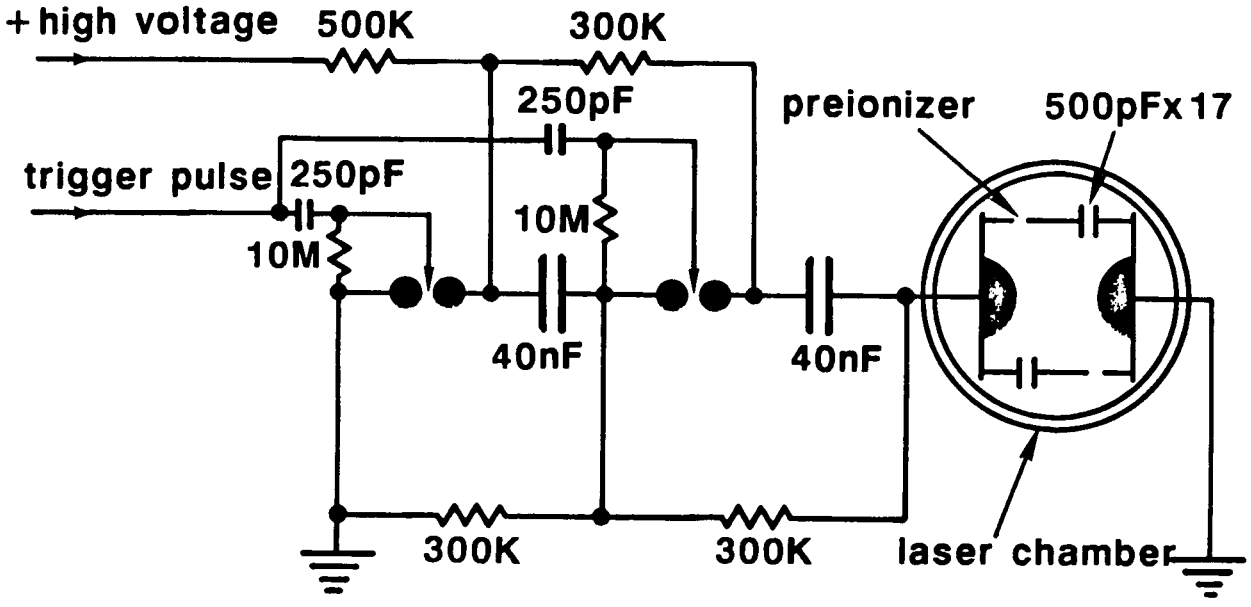

Fig. 1. Electrical circuit diagram of the XeCl excimer laser.

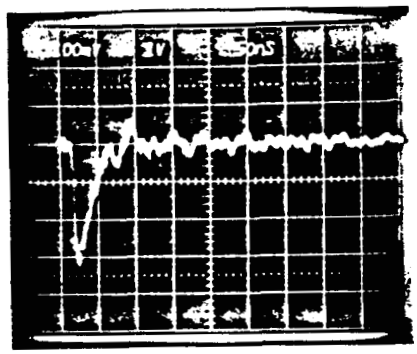

Fig. 2. A typical pulse shape of the XeCl laser output. Three consecutive pulses are overlaped in this picture.

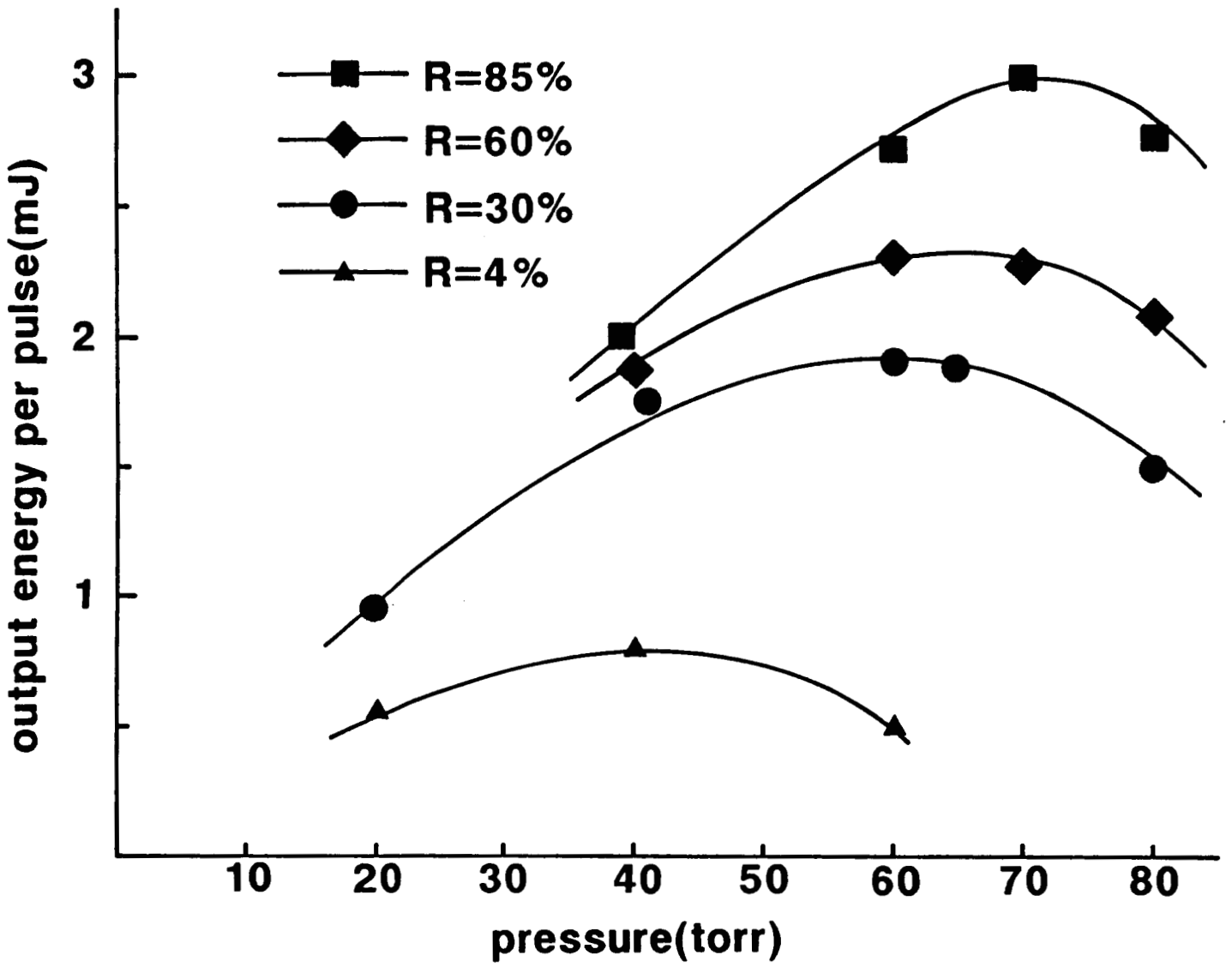

Fig. 3. Iodine laser output energy dependence on the gas fill pressure in the laser cell at each output mirror reflectance. The iodine laser was pumped longitudinally with the XeCl laser of pulse energy 80 mJ.

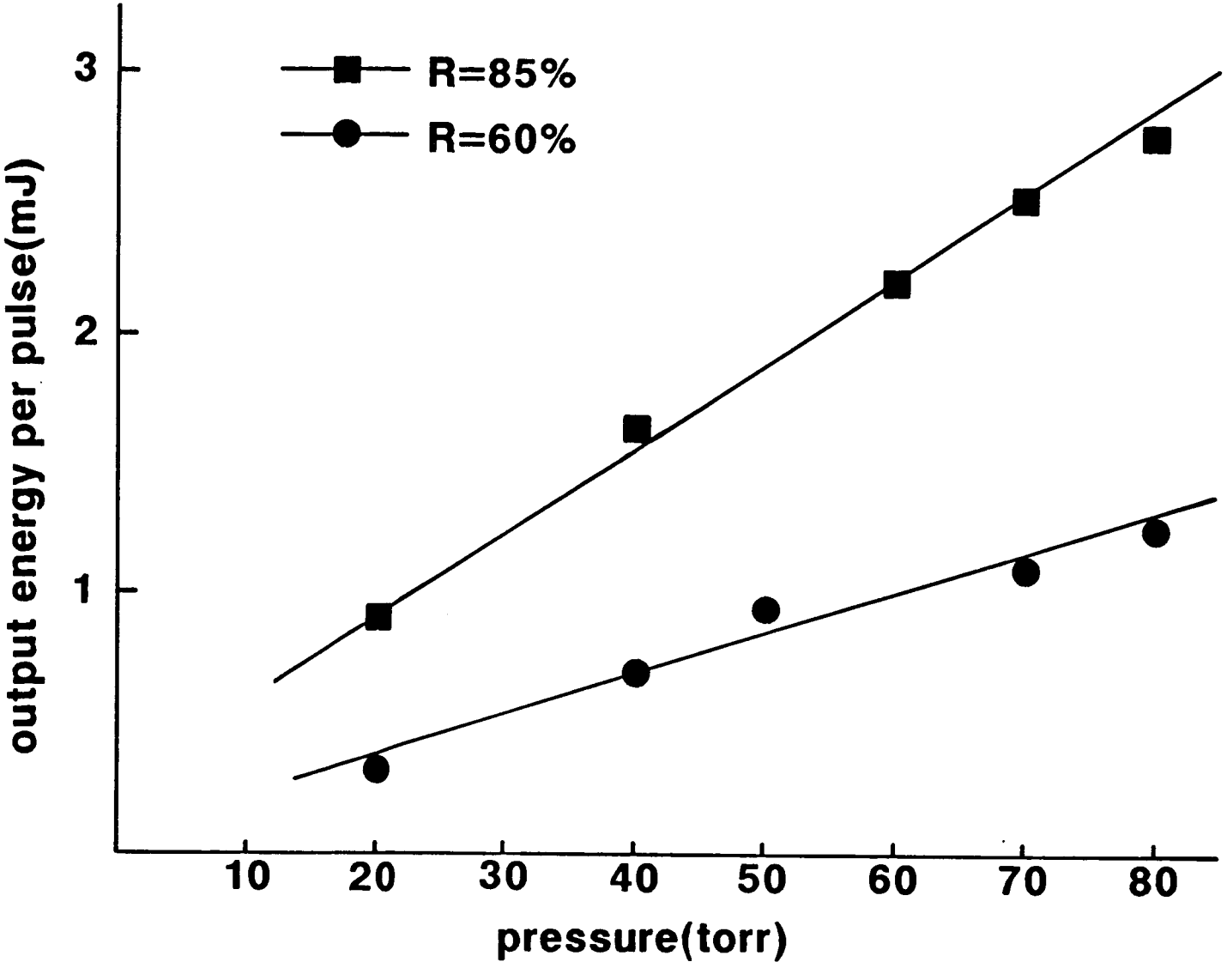

Fig. 4. Iodine laser output energy dependence on the gas fill pressure when the iodine laser was pumped transversely. The pumping energy from the XeCl laser was fixed to 80 mJ.

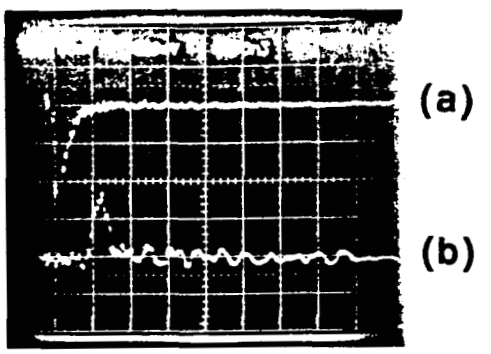

Fig. 5. A typical iodine laser output pulse shape which is compared with the pumping pulse. (a).XeCl pump laser pulse. (b).Iodine laser output pulse.

Kinetic Modeling of a Solar-Pumped Iodine Laser Amplifier System

In pursuant to developing a kinetic model for the iodine solar-simulator pumped power amplifier in the master oscillator power amplifier (MOPA) system, the gain has been calculated for three different lasants (i-C_3F_7I, n-C_4F_9I, and t-C_4F_9I). The kinetic reaction rate coefficients found previously[1,2] by minimizing the error between theoretical calculations and the experimental data for a flashlamp-pumped static fill iodine laser oscillator[3] are used to calculate amplification characteristics of this system. In addition a calculation of the initial inversion ratio for a Q-switched iodine laser is described. Specifically, it has been found that the characteristic parameter which dominates the amount of gain to be obtained from the amplifier is the density of the molecular iodine I_2 as a function of tube length. In addition, the optimum fill pressure for the amplifier or the Q-switched laser is about 10 torr. Later, this model can be used to establish scalability of a solar-pumped iodine laser power generation system to be used for space-to-space power transmission.

The MOPA System

The experiment upon which the modeling effort will be based is the

master oscillator power amplifier (MOPA). This system consists of two stages, the first stage is a XeCl laser pumped iodine laser which will be used as the master oscillator. The output from the oscillator will be amplified in the amplifier system. The modeling effort has been centered about the amplifier stage in an endeavour to understand the processes taking place in the system. The gain of the amplifier has been optimized, and in the future the system will be scaled for space applications.

The iodine laser oscillator uses a XeCl laser as the pumping source. The XeCl laser pumps the oscillator with an output of 80 mJ per pulse and there is no significant reduction in the laser output energy for several hundred discharges. The XeCl laser has a repetition rate of about 5 Hz and the half width (FWHM) of the pulse if about 25 ns with no significant variation in laser pulse shape over extended use. In addition, the output of the XeCl laser is spatially uniform which gives an ideal pumping source for the iodine laser oscillator.

The iodine laser oscillator which is used will be incorporated with the amplifier uses the iodide t-C_4F_9I as a lasant. This lasant has a high degree of chemical reversibility, and the system demonstrated several hundred repetitions without appreciable reduction in laser output energy. The half width (FWHM) of the pulse is about 25 ns and has an output of about 3 mJ[4].

The amplifying medium, i-C_3F_7I or n-C_3F_7I, is pumped continuously by a VORTEK solar simulator in the amplifier. Moreover, the amplifying medium is continuously flowing along the axis of the amplifier tube, thus, the speed

of the flow of the gas and the pressure of the gas can be changed. The VORTEK simulator and the amplifier tube are at the foci of an elliptical cylinder giving a reasonably uniform pumping rate in the amplifying medium. The incident photon flux is to be measured both spatially and as a function of wavelength. The pumping intensity can be varied, to optimize the pumping intensity.

With the demonstrated stability of the laser output when operated as an oscillator, and the pumping intensity spatial uniformity, the amplifier is ideal for kinetic modeling. In addition, the pumping rate of the amplifier is to be found directly as apposed to indirect methods used in previous experiments. This will further reduce the possibility of error introduced into the kinetic model.

Theoretical Considerations

The gain characteristics before the input pulse is sent through the amplifying medium are calculated. The definition of the gain is given by

$$\text{GAIN} = \sigma \int ([I^*] - 1/2\ [I])\ dz\ /\ L_p$$

where σ is the stimulated emission cross-section, L_p the pumping length, and z is the distance down the tube. When the GAIN is less than zero, there is absorption rather than amplification. The input pulse to the amplifier is

about 25 ns, therefore, the energy extraction efficiency is calculated to be about 45%.

The kinetic model used to find the gain is given below as a set of coupled nonlinear differential equations given as

$$d[RI]/dt = K_1 [R] [I^*] + K_2 [R] [I] - \xi_{RI} [RI] - K_4 [R] [RI] + K_5 [R] [I_2]$$

$$d[R]/dt = \xi_{RI} [RI] - K_1 [R] [I^*] - K_2 [R] [I] - 2 K_3 [R]^2 - K_4 [R] [RI] - K_5 [R] [I_2]$$

$$d[R_2]/dt = K_3 [R]^2 + K_4 [R] [RI]$$

$$d[I_2]/dt = C_1 [I] [I^*] [RI] + C_2 [I]^2 [RI] + C_3 [I] [I^*] [I_2] + C_4 [I]^2 [I_2] - \xi_{I2} [I_2] - K_5 [R] [I_2]$$

$$d[I^*]/dt = \xi_{RI} [RI] + \xi_{I2} [I_2] - K_1 [R] [I^*] - C_1 [I] [I^*] [RI] - C_3 [I] [I^*] [I_2] - Q_1 [I^*] [RI] - Q_2 [I^*] [I_2] - A [I^*] - [I^*]/\tau_D$$

$$d[I]/dt = \xi_{I2} [I_2] + Q_1 [I^*] [RI] + Q_2 [I^*] [I_2] + A [I^*] - C_1 [I] [I^*] [RI] - 2 C_2 [I]^2 [RI] - C_3 [I] [I^*] [I_2] - 2 C_4 [I]^2 [I_2] - K_2 [R] [I] + K_4 [R] [RI] + K_5 [R] [I_2] - [I]/\tau_D$$

where ξ_{RI} and ξ_{I2} are the photodissociation rate for the parent molecule RI and molecular iodine I_2 respectively, A is the Einstein coefficient, τ_D is the diffusion time constant, and the reaction rates are given in Table 1. It can be noted that the above differentials do not involve the photon density of the amplifier cavity since the calculation is for the gain before the amplified pulse is considered. Expanding the above total differential to incorporate the flowing gas, the differential of the densities of the gas species $[x_i]$ becomes

$$d[x_i]/dt = \partial[x_i]/\partial t + v\, \partial[x_i]/\partial z \quad i=1,2,\ldots,6$$

where the indicae i indicates the six gas species given above, and v=dz/dt is the flow rate in the z direction. With the introduction of the flowing gas, the linear set of differentials becomes a function of two independent variables, t and z. If a change of variables is made, $\eta=(z/v + t)/2$, $\xi=(z/v - t)/2$ for these of differential equations, they become a function of one independent variable η

$$\partial[x_i]/\partial\eta = F_i([x_i],z,t) \quad i=1,2,\ldots,6$$

where $F_i([x_i],z,t)$ are the functions given above associated with the

differentials of the gas densities [x_l]. Immediately it is recognized that in calculating the gain the velocity of the gas does not change the solution except to indicate where the element of gas along the gain medium is located. Therefore, the solution of the gain is the same at the end of the calculation if both the velocity and gain length are doubled.

In calculating the photodissociation rate for the different gas species, the average fractional attenuation is given as a function of radial distance by[2]

$$F_A(P_o) = 2 \int r\, F(y,P_o)\, dr \,/\, R^2$$

where $y = R - r$, and r is the radial distance in the tube, R is the radius of the tube, P_o is the pressure of the medium in torr, and n is the gas number density for one torr. The relative fractional attenuation of the pump light in the tube is given by[5,7]

$$F(y,P_o) = f \exp(-\, P_o\, n\, \sigma_0\, y) + (1- f) \exp(-.223\, P_o\, n\, \sigma_0\, y)$$

which is a function of the fractional absorption[5] near line zero f, and the absorption cross-section for the different gasses σ_0. Since the photodissociation rate for on solar constant has been calculated previously, the photodissociation rate[2,5] relative to i-C_3F_7I is used, 85% for n-C_4F_9I and 83% for t-C_4F_9I. In addition to the absorption of the light used to pump the

amplifier being a function of P_o, the stimulated emission cross-section is a function of $P_o 7$. Figure 1 indicates the dependence of the stimulated emission cross-section on the gas pressure.

Figure 1.

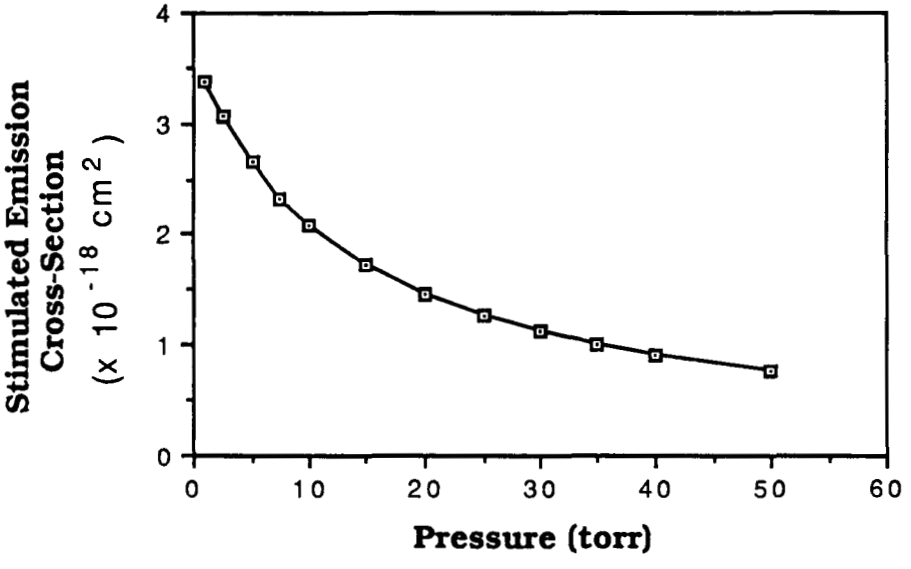

Using these values for the stimulated emission cross-section and the relative attenuation of light, the system can be understood and subsequently optimized by looking at the gain profile for radial and axial distances in the gain medium. This is done here by examining the dependence of the gain on the pressure of the amplifying medium, pumping intensity, and tube radii.

Computational Results

In order to investigate the amplification characteristics of the MOPA system, the GAIN profile of the amplifier is calculated as a function of pressure for various pumping intensities. In this case the tube is assumed to have a diameter of 2 cm. In addition, the gain is given as a function of tube radii for different pressures for a pumping intensity of 1500 SC. For all the gasses the flow speed is assumed to be seven meters per second. These calculations were done using the kinetic coefficients[2] for the gasses i-C_3F_7I, n-C_4F_9I, and t-C_4F_9I given in Table I.

In figures 2, 4, and 6 the gain is given as a function of gas pressure for various pumping intensities, and it can be seen that the gain is a maximum at about 10 torr. In figures 3, 5, and 7, the corresponding maximum $[I_2]$ divided by the parent molecule density [RI] is given and shows the dominant role I_2 has upon the gain profile; i. e., as the pressure increases the $[I_2]$ increases, such that, even though the pumping intensity increases, the gain decreases. Furthermore, since the kinetic reaction rate for t-C_4F_9I is much less than that of i-C_3F_7I for producing the dimer R_2, the maximum $[I_2]$ is five times less for t-C_4F_9I which means that I_2 plays a lesser role in the gain profile. The gain decreases as the pressure increases above 10 torr,but there is a wider range of pressures for the optimum gain.

Figures 8 through 13 give the gain profile as a function of axial distance for different pumping intensities, pressures, and gasses. The integral of the gain as a function of distance is given along with the gain for the element of gas at a specific axial distance. The inflection point of the gain integral is

where the inversion density is negative. At this point, the $[I_2]$ is effectively quenching enough upper iodide states to create a negative inversion. In figures 8 through 11, it is shown that there is no dramatic increase in $[I_2]$ for the i-C_3F_7I pressure less than 15 torr. It can also be seen as the pumping intensity is increased, the inflection point is earlier in the tube. Therefore, increasing the flow rate would be beneficial at the higher pressures, moving the I_2 out quickly. On the other hand, in figures 12 and 13, for the gas t-C_4F_9I, here the inversion density is almost linear as a function of axial distance, except at the higher pressures. At higher pressures, again, there is an inflection point for the inversion density, but it is not as pronounced. In the case of the t-C_4F_9I, increasing the flow rate would be less beneficial compared with the i-C_3F_7I gas.

In figures 14 and 15 the average gain is given as a function of pressures for different tube radii, as well as the corresponding average attenuation fraction used for the calculation. For zero radius there is assumed to be no absorption. It can be discerned that there is a point of diminishing returns gotten from increasing the tube radius since the average gain decreases as the tube diameter increases (figure 15). Also in figure 16 the is a gain profile for a pressure of 10 torr using $F(x,P_o)$ as the attenuation function. This type of information is important for scaling the system.

Figure 16.

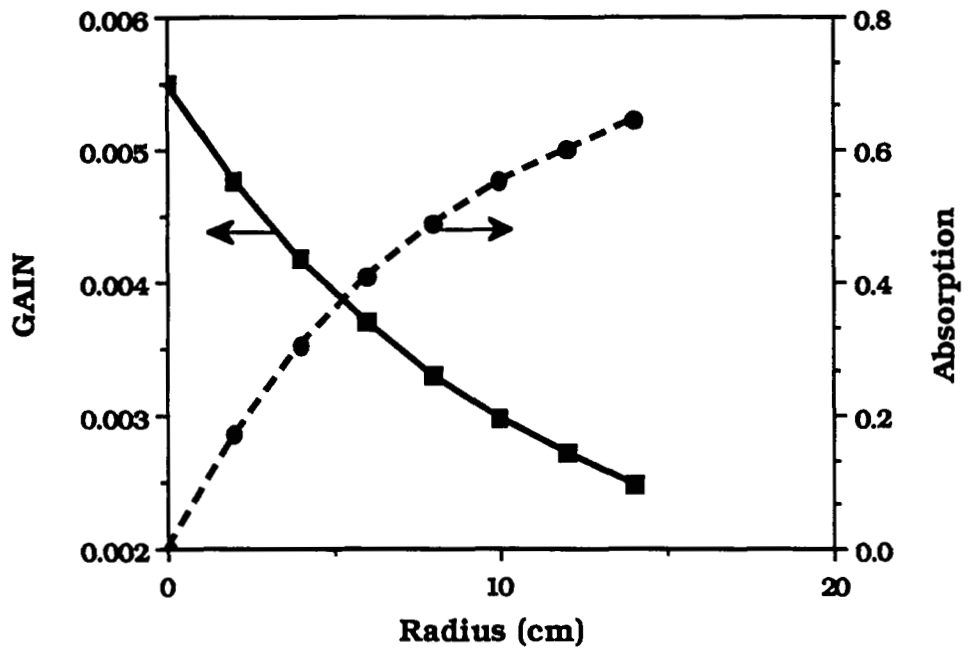

Q-Switched Laser

There are many applications for Q-switched, gain switched lasers in a space environment. A Q-switched laser is one in which the cavity feed back in a laser oscillator is temporarily interrupted and then restored. The calculation is for a continuously-pumped, flowing, iodine Q-switched laser. The initial inversion ratio is defined as the ratio of the population inversion just after switching to the threshold inversion just after switching[8]. This ratio is given as

$$r = c\,\sigma\,\tau_c \int ([I^*] - 1/2\,[I])\,dz \,/\, L_p$$

where c is the speed of light, τ_c is the optical time constant defined as[5]

$$\tau_c = - 2 (L_c / c) / \ln(R_1 R_2)$$

where L_c is the cavity length, and R_1 and R_2 are the mirror reflectivities. Therefore, when r equals one the total loss in the system is equal to the gain. The calculation is for a cavity length of 80 cm, tube diameter of 2 cm, mirror reflectivities of 85% and 98%, and the gain length for the pumping cavity L_p is 20 cm. The contribution the inversion density down stream of the pumping cavity has upon the population inversion just after switching is neglected.

In figure 17 the profile of the initial inversion ratio for the lasant i-C_3F_7I is given as a function of lasant pressures and pumping intensities. It is observed that the gain profile for the amplifier (figure 2) and the initial inversion ratio are the same except for the constants τ_c and c. In addition, the peak $[I_2]$ is the same for the different pressures and pumping intensities, and since the calculations are the same the gas densities as a function of tube length are identical. Here, the physical parameters for the lasant and the tubes of the systems are the same, which means that the calculations of the two profiles are identical. If the amplifier is triggered before the tube is refilled, or the Q-switched laser is switched on before the

laser tube is replenished with fresh gas; there may not be a similarity between the two profiles.

Summary and Future Plans

To summarize, the $[I_2]$ along the axis of the tube affects seriously the gain profile. For the gas i-C_3F_7I at the higher pressures because of the $[I_2]$, as the pumping intensity increases the gain will decrease, and at these higher pressures an increase in flow velocity will increase the gain. In addition, there is an optimum pressure for the amplifying medium for a specific flow velocity.

These gain calculations is the first step in developing a kinetic model of the MOPA system. The steps to be included in the further development the model are, first, the square pulse amplification in the amplifier, then time dependence to the pulse, and later pulses at a higher repetition rate. This kinetic model will establish a basis to compare theory and experiment in order to establish a scaling law for a solar-pumped space-based iodine laser amplifier chain which will be used for the generation and transmission of power.

References

1. L. V. Stock, NASA Progress Report of NAG-1-441, November 1986.

2. L. V. Stock and J. W. Wilson, "A Kinetic Model for a Solar-Pumped Iodine Laser," ILS-III Conference, November 1987.

3. B. M. Tabibi, M. H. Lee, J. H. Lee, and W. R. Weaver, Proceedings of the International Conference on Lasers '86, pp. 144-149 (1986).

4. In Heon Hwang and Kwang S. Han, and J. H. Lee, "XeCl Laser Pumped Iodine Laser Using t-C_4F_9I," Submitted to Optics Communications, August 1988.

5. J. W. Wilson, Y. Lee, W. R. Weaver, D. H. Humes, and J. H. Lee, NASA TP-2241 (1984).

6. John Heinbockel, NASA Progress Report of NAG-1-757, January 1988.

7. J. H. Lee, J. W. Wilson, T. Enderson, D. H. Humes, W. R. Weaver, and B. M. Tabibi, Optics Comm. **53**. 367 (1985).

8. A. E. Siegman, **Lasers**, University Science Books, Mill Valley, CA,(1986), Chapter 26.

List of Figures

TABLE I. - Reaction rate coefficients and their associated reactions for the gasses.

Reactions	Symbols	i-C_3F_7I	n-C_4F_9I	t-C_4F_9I
$R + I^* \rightarrow RI$	K_1	$.1633 \times 10^{-11}$	$.7499 \times 10^{-12}$	$.9569 \times 10^{-12}$
$R + I \rightarrow RI$	K_2	$.1336 \times 10^{-10}$	$.9884 \times 10^{-11}$	$.2750 \times 10^{-10}$
$R + R \rightarrow R_2$	K_3	$.4385 \times 10^{-11}$	$.6065 \times 10^{-11}$	$.7576 \times 10^{-12}$
$R + RI \rightarrow R_2 + I$	K_4	$.7663 \times 10^{-16}$	$.7762 \times 10^{-16}$	$.4755 \times 10^{-16}$
$R + I_2 \rightarrow RI + I$	K_5	$.1783 \times 10^{-11}$	$.2240 \times 10^{-10}$	$.1117 \times 10^{-11}$
$I^* + I + RI \rightarrow I_2 + RI$	C_1	$.1095 \times 10^{-32}$	$.8688 \times 10^{-33}$	$.3638 \times 10^{-32}$
$I + I + RI \rightarrow I_2 + RI$	C_2	$.5970 \times 10^{-31}$	$.2182 \times 10^{-31}$	$.4206 \times 10^{-31}$
$I^* + I + I_2 \rightarrow I_2 + I_2$	C_3	$.8000 \times 10^{-31}$	$.8000 \times 10^{-31}$	$.8000 \times 10^{-31}$
$I + I + I_2 \rightarrow I_2 + I_2$	C_4	$.3933 \times 10^{-29}$	$.3933 \times 10^{-29}$	$.3933 \times 10^{-29}$
$I^* + RI \rightarrow I + RI$	Q_1	$.1122 \times 10^{-15}$	$.3006 \times 10^{-16}$	$.1231 \times 10^{-15}$
$I^* + I_2 \rightarrow I + I_2$	Q_2	$.3400 \times 10^{-10}$	$.3400 \times 10^{-10}$	$.3400 \times 10^{-10}$

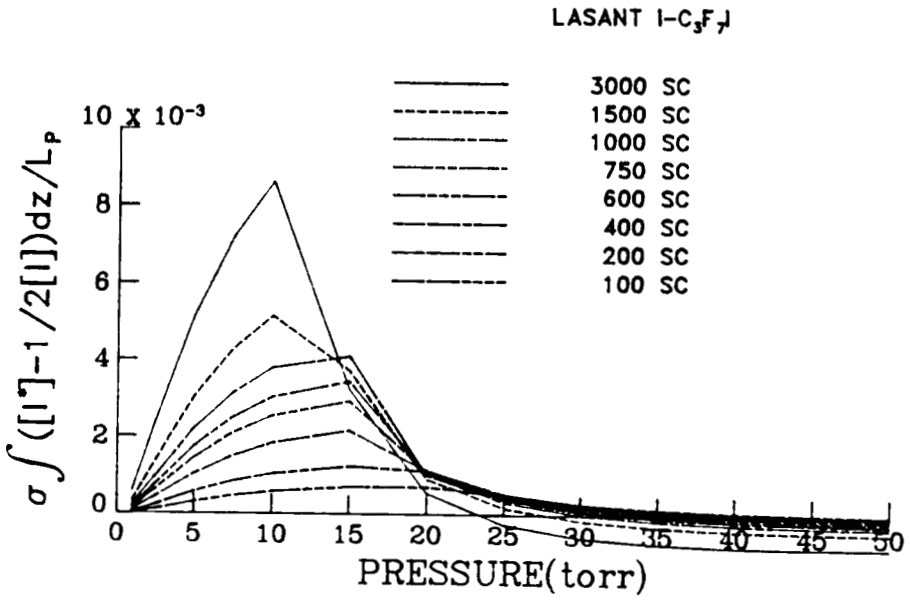

Figure 2.

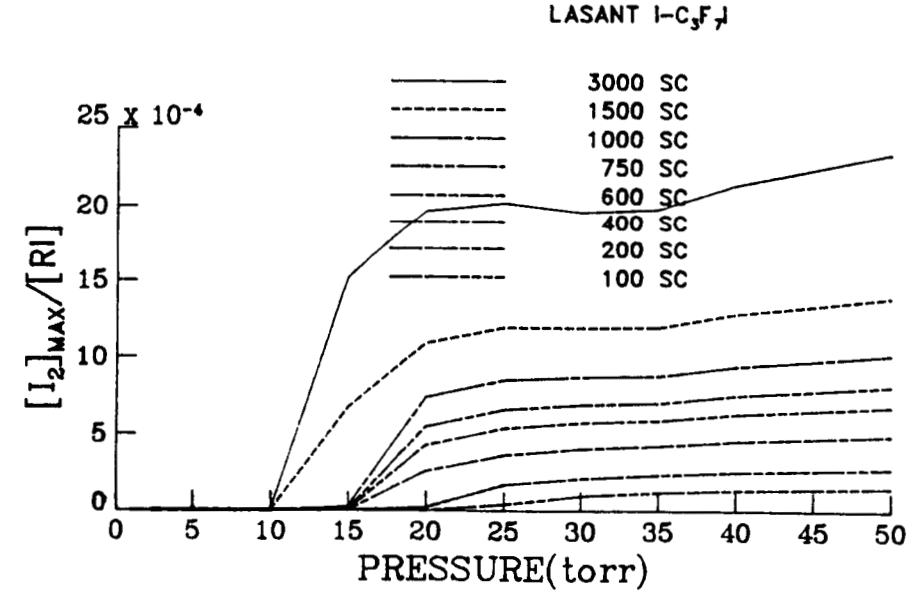

Figure 3.

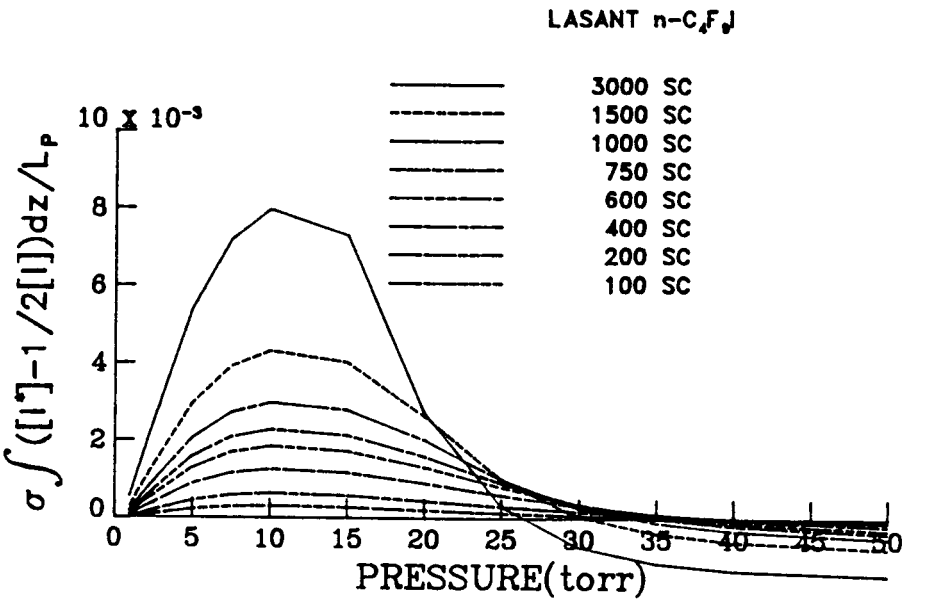

Figure 4.

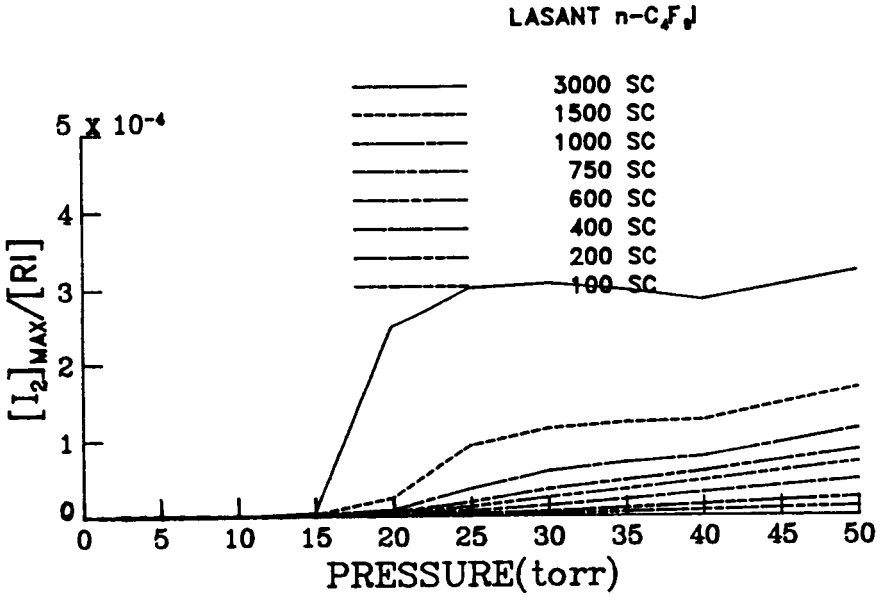

Figure 5.

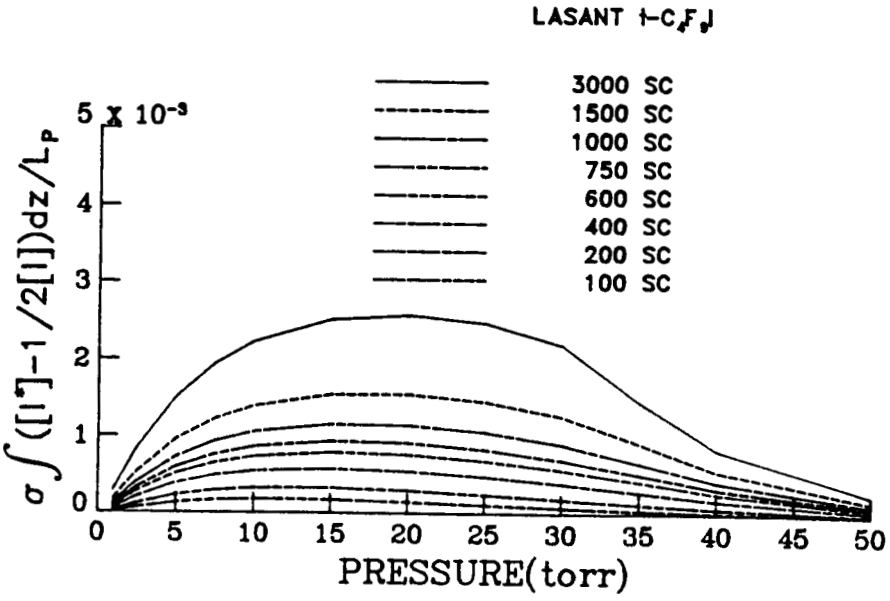

Figure 6.

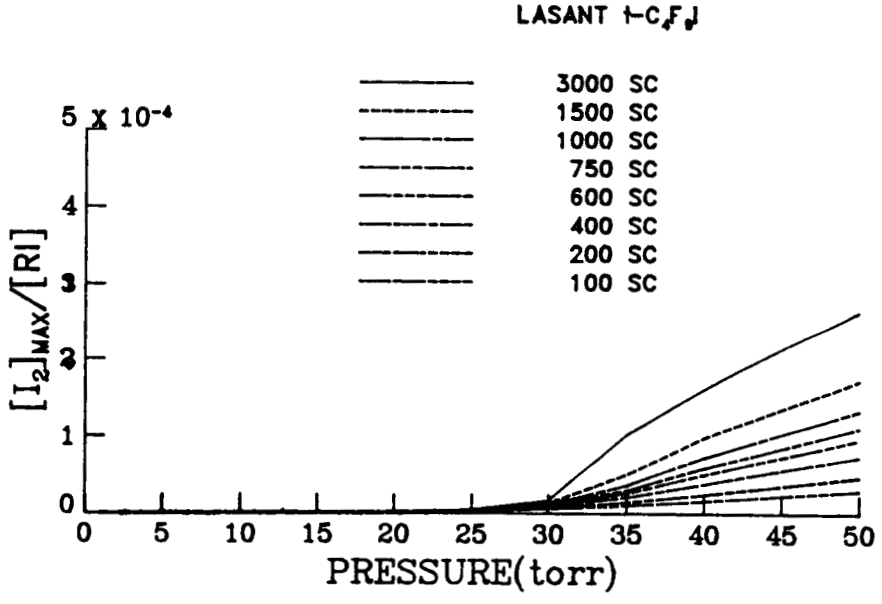

Figure 7.

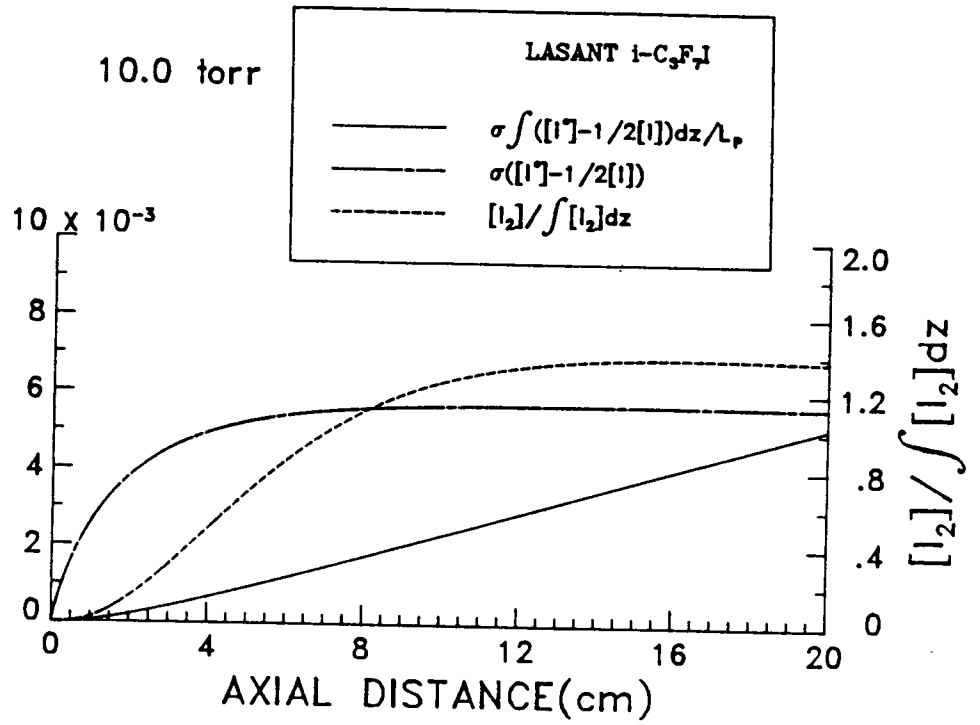

Figure 8.

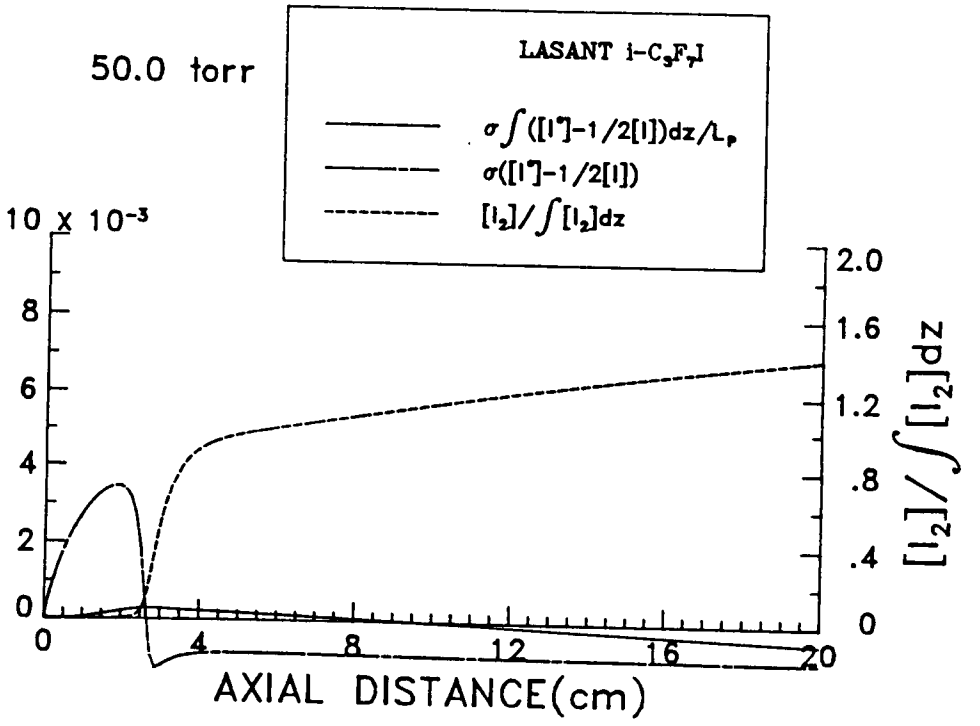

Figure 9.

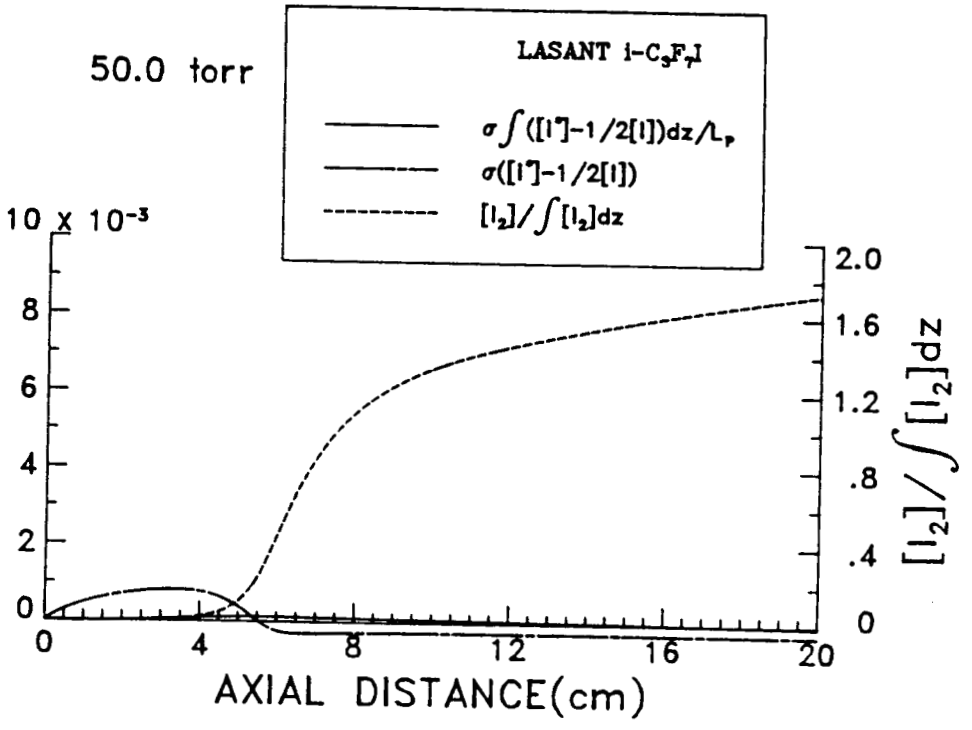

Figure 10.

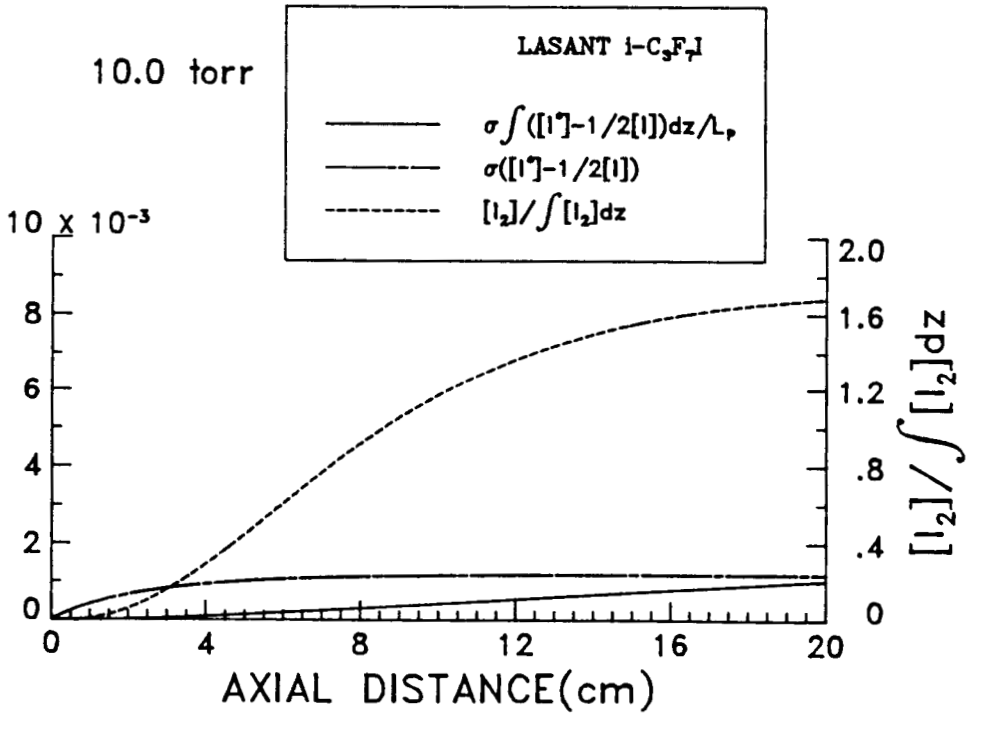

Figure 11.

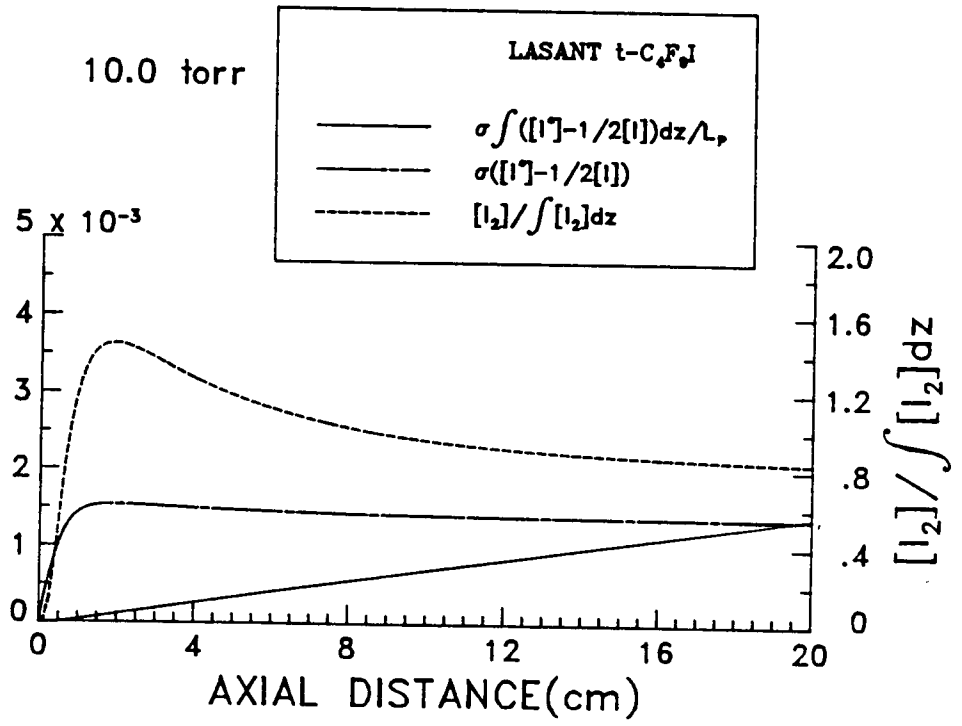

Figure 12.

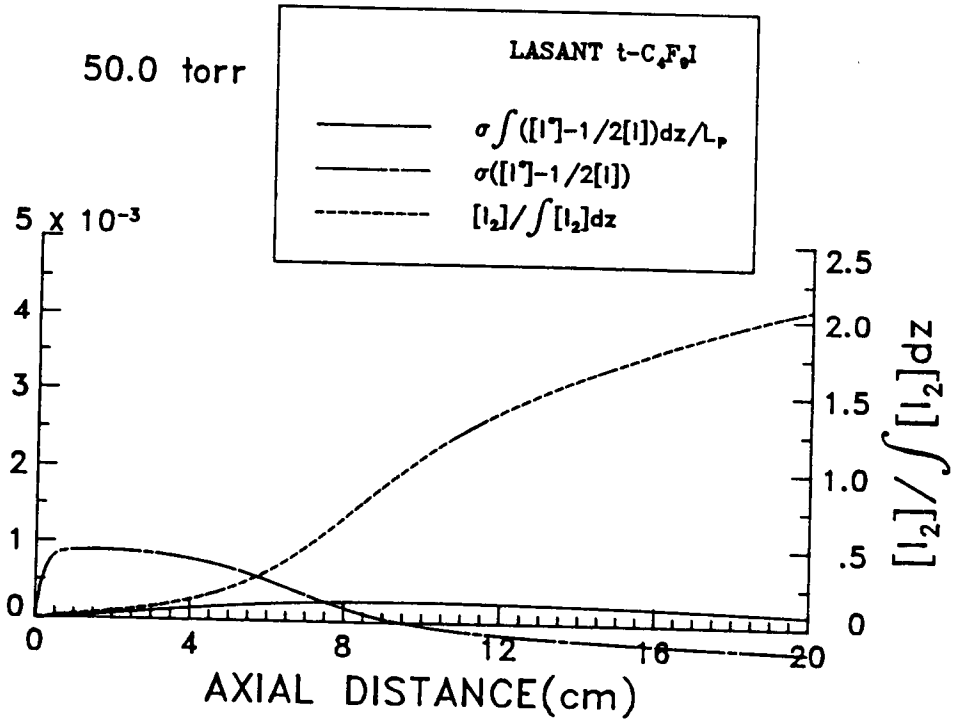

Figure 13.

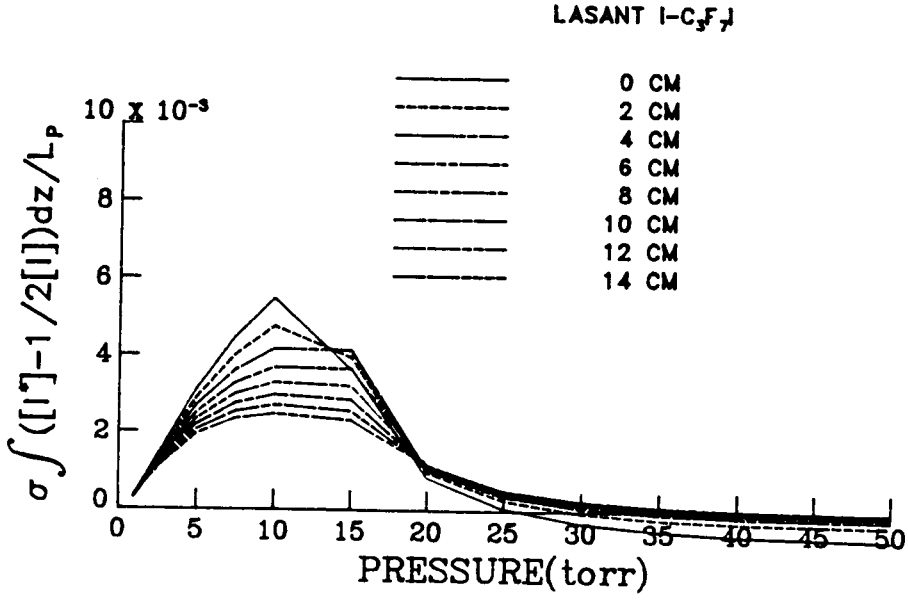

Figure 14.

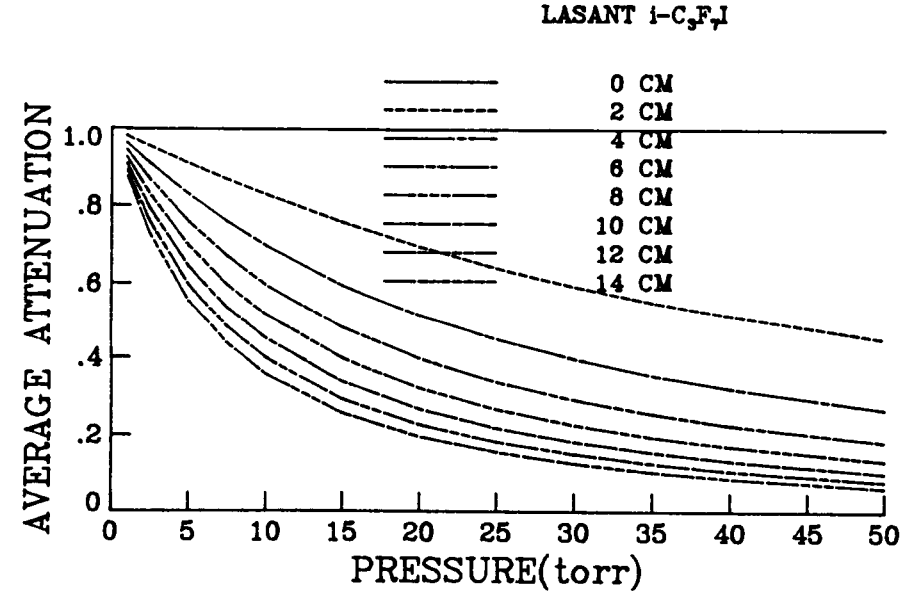

Figure 15.

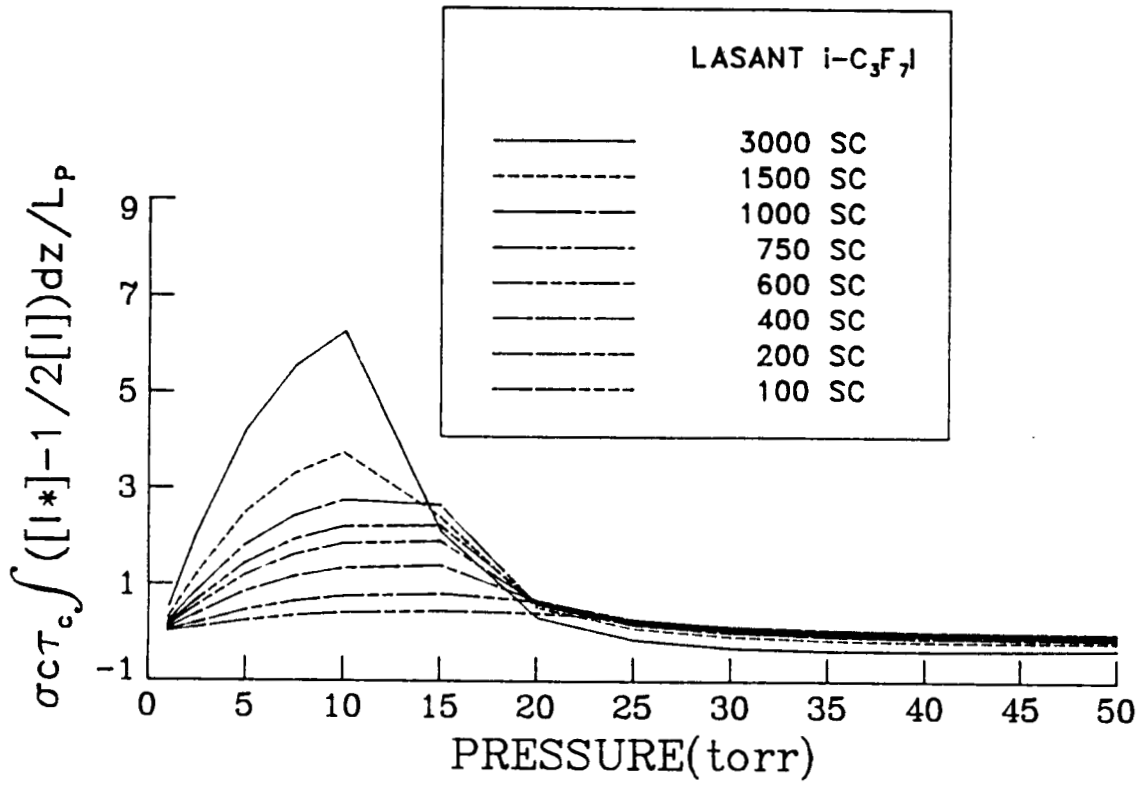
LASANT i-C3F7I
3000 SC
1500 SC
1000 SC
750 SC
600 SC
400 SC
200 SC
100 SC
σcτc∫([I*]-1/2[I])dz/Lp
9
7
5
3
1
-1
0
5
10
15
20
25
30
35
40
45
50
PRESSURE(torr)

Figure 17.